Nutrition & Diabetes

https://doi.org/10.1038/s41387-026-00440-y

Article in Press

Insulin resistance drives GGT elevation in MASLD with diabetes: evidence from clinical cohorts, mendelian randomization and functional genomics

Received: 10 June 2025

Revised: 18 May 2026

Accepted: 2 June 2026

Cite this article as: Mandal, A., Chatterjee, A., Ganguly, D. *et al.* Insulin resistance drives GGT elevation in MASLD with diabetes: evidence from clinical cohorts, mendelian randomization and functional genomics. *Nutr. Diabetes* (2026). https://doi.org/10.1038/s41387-026-00440-y

Ayan Mandal, Ankita Chatterjee, Debopriyo Ganguly, Bandana Mondal, Analabha Basu & Priyadarshi Basu

Title:

Insulin Resistance Drives GGT Elevation in MASLD with Diabetes: Evidence from Clinical Cohorts, Mendelian Randomization and Functional Genomics

Running Title:

Insulin Resistance and GGT in MASLD with Diabetes

Authors: Ayan Mandal[1, 2,*], Ankita Chatterjee[3], Debopriyo Ganguly [1, 2], Bandana Mondal [1, 2], Analabha Basu[1, 2], Priyadarshi Basu[1, 2,#]

[1] Biotechnology Research Innovation Council-National Institute of Biomedical Genomics (BRIC-NIBMG), Kalyani, India.

[2] Regional Centre for Biotechnology, Faridabad, India.

[3] John C. Martin Center for Liver Research and Innovations, Kolkata, India.

[*] First Author

[#] Corresponding Author

Corresponding Author:

Dr. Priyadarshi Basu

Biotechnology Research Innovation Council–National Institute of Biomedical Genomics (BRIC–NIBMG)

Kalyani, India

Email: pb1@nibmg.ac.in

Abstract

Background:

Metabolic dysfunction-associated steatotic liver disease (MASLD) and type 2 diabetes (T2D) commonly occur together and are linked by shared factors like insulin resistance and excess liver fat. While enzymes such as ALT and AST are routinely measured in these conditions, the clinical significance of gamma-glutamyl transferase (GGT) remains less well understood.

Objective:

To investigate the relationship between GGT, insulin resistance, and MASLD using integrative approaches combining clinical data, Mendelian Randomization (MR), and functional genomics.

Method:

A hospital-based cohort (N = 498) was analyzed for MASLD and T2D status alongside liver enzymes and insulin resistance (HOMA-IR). Findings were validated in the NHANES 2017–2020 dataset (N = 2586). Univariable and multivariable MR analyses were performed using GWAS summary statistics for fasting insulin, glycemic traits, and percentage liver fat to assess their potential causal effects on GGT. Functional annotation of GGT-associated variants was conducted using FUMA.

Results:

Individuals with both MASLD and T2D exhibited significantly elevated GGT and HOMA-IR levels compared to those with either condition alone. MR analyses demonstrated a potential causal effect of genetically predicted fasting insulin on GGT, independent of other metabolic traits. Functional enrichment analysis revealed involvement of insulin signaling and lipid

metabolism pathways. Tissue expression highlighted predominant liver and pancreatic expression of GGT-associated genes.

Conclusion:

These findings suggest that insulin resistance may contribute more strongly to GGT elevation in MASLD than hepatic fat accumulation, though the comparatively weak instrument strength for liver fat in the multivariable model warrants cautious interpretation of this comparison. Genetically predicted fasting insulin showed a potential causal effect on GGT independent of other metabolic traits. GGT appears to reflect underlying metabolic dysfunction, particularly insulin resistance; however, further prospective and interventional studies are required before its role as a predictive or clinically actionable biomarker can be established.

1. Introduction

Metabolic dysfunction-associated steatotic liver disease (MASLD) is a common non-viral chronic liver disorder marked by excess hepatic fat (>5% hepatocytes) (ref. 1). MASLD encompasses a spectrum of liver diseases ranging from simple steatosis, which is considered to be a benign condition, to metabolic dysfunction-associated steatohepatitis (MASH), which is characterized by liver inflammation and fibrosis (ref. 1). MASH may progress to cirrhosis and hepatocellular carcinoma (HCC) (ref. 2, 3). The prevalence of MASLD has increased in recent years, affecting 25% of the global population. In India, it ranges from 28-53% among the urban population, suggesting a higher disease burden (ref. 4, 5). Type 2 Diabetes (T2D) is a metabolic disorder characterized by hyperglycemia resulting from Insulin Resistance (IR) and impaired insulin secretion (ref. 1, 6). MASLD and T2D frequently coexist, and their relationship is considered bidirectional, with each condition increasing the risk and severity of the other (ref. 6–10). Type 2 Diabetes promotes MASLD progression to cirrhosis and increases the risk of liver-related mortality by two to threefold (ref. 11). Prediabetes, an intermediate hyperglycemic state preceding T2D (ref. 12), is also associated with a high prevalence of MASLD (ref. 13, 14). Insulin Resistance (IR) is a phenomenon that is critical for the development of MASLD in the presence or absence of definite T2D (ref. 15). It precedes overt hyperglycemia and is highly prevalent among individuals with MASLD (ref. 16–18). While the epidemiological association between MASLD and glycemic traits is well established, it remains unclear whether insulin resistance and related metabolic traits causally drive liver disease progression or simply reflect shared metabolic dysregulation.

Gamma-glutamyl transferase (GGT) is a liver-derived enzyme widely used as a clinical marker of hepatocellular injury (ref. 19). Beyond reflecting liver damage, elevated GGT levels have

been associated with insulin resistance and type 2 diabetes and cardiometabolic risk (ref. 20-22). However, whether GGT elevation reflects hepatic fat accumulation per se or is mechanistically linked to systemic insulin resistance remains uncertain.

To date, most studies examining the relationship between glycemic traits and MASLD have been observational, limiting causal inference. The specific contribution of insulin resistance independent of hepatic fat accumulation, to GGT elevation and disease severity has not been clearly delineated.

To address these gaps, we combined clinical phenotyping with Mendelian Randomization (MR), a genetic epidemiology approach that leverages genetic variants as instrumental variables to infer causality. We aimed to compare MASLD severity across normoglycemia, prediabetes and T2D and to evaluate whether genetically predicted insulin resistance related traits and hepatic fat exert causal effects on GGT levels. By integrating clinical and genetic approaches, this study seeks to clarify whether GGT serves primarily as a marker of hepatic fat accumulation or as a reflection of systemic insulin resistance.

2. Materials and Methods:

2.1 Study Participants:

All participants in the discovery cohort were of Indian origin and recruited from SSKM Hospital, Kolkata. Clinical histories were collected as described previously (ref. 23). Individuals with alcohol use or secondary steatosis causes were excluded. Anthropometric data and fasting blood samples were collected. Lipid profile, liver function tests and diabetes markers (FBG, FI, HbA1c) were measured using standard procedures. Insulin sensitivity was estimated using the homeostasis model of insulin resistance (HOMA-IR) (ref. 24) in 391 individuals. Liver fat was

assessed by abdominal ultrasonography (USG) and proton MR spectroscopy (H1-MRS) in all participants.

2.2 Validation cohort (NHANES 2017-2020 Pre-pandemic data)

To validate our findings, we used NHANES 2017–2020 pre-pandemic data which represents a nationally representative, multi-ethnic U.S. population including Mexican American, Hispanic, Non-Hispanic White, Non-Hispanic Black, Non-Hispanic Asian, and other racial/ethnic groups. 3729 adults with complete elastography, glucose, insulin, cardiometabolic, and liver test data were initially included. 1143 were excluded due to potential liver disease (e.g., hepatitis B/C, or alcohol use). Ultimately, 2586 individuals were included. Exclusion details are shown in Supplementary Figure 1A.

2.3 Categorizing the study participants based on MASLD and Diabetes status

The 498 participants were divided into MASLD (n = 312) and no-MASLD (n = 186) groups based on USG and MRS findings, along with the presence of at least one cardiometabolic risk factor per the Delphi consensus (ref. 6). USG grade 0 and/or MRS fat < 5% defined the no-MASLD group; USG grade ≥ 1 and/or MRS fat > 5% with any of five cardiometabolic criteria defined MASLD. Groups were further classified as ND, PD, or D using American Diabetic Association (ADA) criteria: ND (FBG < 100 mg/dL, HbA1c < 5.7%), PD (FBG 100-125 mg/dL, HbA1c 5.7-6.4%), and D (FBG > 125 mg/dL, HbA1c > 6.4%) (Figure 1A).

2.4 MASLD and Diabetes classification in NHANES data

The presence of hepatic fat deposition was evaluated using elastography based controlled attenuated parameter (CAP), where a CAP score exceeding 275 dB/m indicated the presence of hepatic steatosis (ref. 25). The diagnosis of MASLD included the presence of hepatic steatosis

along with either of the five cardiometabolic criteria following the multi-society Delphi consensus as previously mentioned. Diabetes classification was done following the American Diabetic Association (ADA) norms as previously mentioned. The detailed study design is presented in Supplementary Figure 1B.

2.5 Histopathological evaluation

Liver tissue samples were available for a subset of MASLD individuals (n = 138) from a previously characterized cohort described by Chatterjee et al. (ref. 23). In that study, liver biopsy was performed as part of routine clinical evaluation in patients with suspected MASLD to confirm diagnosis and assess disease severity, including steatosis, inflammation, hepatocyte ballooning, and fibrosis. A part of the tissue was preserved in 10% Formalin solution and embedded in paraffin blocks for histopathological evaluation. The paraffinized samples were sectioned by microtome and haematoxylin and eosin staining was performed for morphological evaluation. The histological evaluation was performed by a single examiner, as mentioned previously (ref. 23). Disease severity was determined through NAFLD Activity Score (NAS) (ref. 26, 27), which is the sum of steatosis score, hepatocyte ballooning and lobular inflammation score. The fibrosis score was also calculated following the NASH-CRN criteria (ref. 27) to determine the degree of fibrosis.

2.6 Clinicopathological characteristics and Liver Histopathology Scores

Clinicopathological characteristics like lipid profile, liver damage markers, albumin, globulin, creatinine, fasting Insulin were compared between the ND, PD and D Groups in MASLD as well as no-MASLD group to compare how they change in people with MASLD, with increasing severity of Type 2 Diabetes. Liver histopathology scores like Steatosis Score (SS), Hepatocyte

Ballooning Score (HBS), Lobular Inflammation Score (LIS), Fibrosis Score (FIB), Portal Inflammation Score (PIS) and NAFLD Activity Score (NAS) were compared to check the proportion of individuals showing higher severity of liver damage based on histopathology scores among the different subgroups.

2.7 Mendelian Randomization Analysis

2.7.1 Study Design and Data source

This study was designed according to the STROBE-MR guidelines (ref. 28) and the completed checklist is provided as a supplementary file. Mendelian Randomization analysis relies on three core assumptions: (i) relevance (genetic variants are associated with the exposure), (ii) independence (variants are not associated with confounders), and (iii) exclusion restriction (variants influence the outcome only through the exposure). For our bidirectional two-sample Mendelian Randomization (MR), we used GWAS summary statistics to investigate the causal relationship between IR-related traits and Gamma-Glutamyl Transferase (GGT) levels. Specifically, we assessed the causal effects of fasting insulin (FI), fasting blood glucose (FBG), glycated hemoglobin (HbA1c), and percentage liver fat (LF) on GGT levels, as well as in the reverse direction, evaluating the causal influence of GGT on these metabolic traits.

The selected exposures were chosen to represent complementary aspects of insulin resistance, glycemic regulation, and hepatic fat accumulation. Fasting insulin, derived from large-scale GWAS in non-diabetic populations, is widely used as a genetic proxy for systemic insulin resistance (ref. 29). Fasting blood glucose and HbA1c reflect short-term and long-term glycemic status respectively (ref. 30). Percentage liver fat was included to distinguish the potential contribution of hepatic steatosis from systemic insulin resistance in driving GGT levels.

For FI, FBG, and HbA1c, we obtained GWAS summary statistics from the Meta-Analysis of Glucose- and Insulin-related traits Consortium (MAGIC) (ref. 31), which included 151,013; 200,622 and 146,806 European-ancestry individuals, respectively. The corresponding NHGRI-EBI GWAS Catalog accession numbers are GCST90002238 (fasting insulin), GCST90002232 (fasting glucose), and GCST90002244 (HbA1c). The summary statistics for MRI-derived liver fat percentage was obtained from a GWAS conducted in 32,858 European-ancestry individuals from the UK Biobank (ref. 32, accession GCST90016673).

For the outcome variable GGT, we used GWAS summary statistics based on 361,194 White-British participants from the UK Biobank, as released by the Neale Lab (https://www.nealelab.is/uk-biobank). In the reverse MR analysis, we examined whether genetically predicted GGT levels influenced FI, FBG, HbA1c and percentage liver fat.

Since fasting insulin, fasting glucose, HbA1c, and liver fat are metabolically interrelated traits and have been shown in prior studies to be phenotypically correlated and linked to insulin resistance (ref. 33, 34), we performed multivariable MR analyses to isolate the direct effect of each exposure conditional on the others.

2.7.2 Instrument Variable selection

Single Nucleotide Polymorphisms (SNPs) for each variable were selected based on a genome-wide significance threshold $P < 5 \times 10^{-8}$. Quality control steps were implemented on these SNPs to select eligible instrument variables (IVs). Firstly, palindromic alleles (example: A/T or G/C) were excluded. Secondly, SNPs for each variable were clumped with a Linkage Disequilibrium (LD) threshold set at $r^2 < 0.001$ and a clumping window of 10000 kb, to select only independent SNPs as IVs. LD was estimated based on the European-based 1,000 Genome Projects reference

panel (ref. 35). Thirdly, the MR pleiotropy residual sum and outlier (MR-PRESSO) test was applied to detect potential horizontal pleiotropy and to eliminate the effects of pleiotropy by removing outliers (ref. 36). Instrument strength was assessed using the F-statistic, and all selected SNPs demonstrated F-statistics > 10, indicating adequate instrument strength. Detailed SNP-level information, including the number of instruments per exposure and corresponding F-statistics, is provided in Supplementary Table 1.

Unlike univariate MR, where IVs were selected independently for each exposure, in MVMR, SNPs in LD with variants from another exposure were removed to ensure statistical independence. As a result, the number of SNPs included in MVMR was lower than in the univariate analysis. The LD threshold and the clumping window used for MVMR analysis were same as the univariable MR analysis ($r^2 < 0.001$ and 10000 kb). The SNPs used for MVMR are mentioned in Supplementary Table 1.

2.7.3 Statistical Analysis for MR

Since multiple IVs were used for each variable, random-effects inverse variance weighted (IVW) test was used (ref. 37) along with MR-Egger regression (ref. 38) and weighted median method (ref. 39). The IVW method assumes no horizontal pleiotropy (ref. 37). The MR-Egger assumes the presence of pleiotropy in > 50% SNPs (ref. 38). The weighted median method assumes the presence of pleiotropy in < 50% SNPs (ref. 39). The IVW method is reported to be slightly more powerful than the others under certain conditions (ref. 39). Therefore, the results were mainly based on the IVW method, with the other two methods serving as its complements.

To assess robustness of significant results, we performed several sensitivity analyses. The potential heterogeneity was examined by the Q test in the IVW test and the MR-Egger

regression. The intercept of the MR-Egger regression test was used to provide an estimate of the degree of directional pleiotropy. Meanwhile, the leave-one-out analysis was performed to determine whether the causal signal was driven by one SNP. Steiger directionality filtering was performed to confirm that the selected genetic variants explained greater variance in the exposure than in the outcome, thereby supporting the assumed causal direction. In the multivariable MR framework, conditional instrument strength was assessed using Sanderson–Windmeijer conditional F-statistics (ref. 40) as implemented in the MVMR package. Conditional F-statistics greater than 10 were considered indicative of adequate instrument strength, consistent with established methodological recommendations. All statistical analyses were conducted using R (v4.0.3) using TwoSampleMR (v0.6.30) (ref. 41), MendelianRandomization (v0.10.0) (ref. 42) and MVMR (v0.4.2) (ref. 40) packages.

2.8 Functional Mapping and Annotation (FUMA) Analysis

Functional annotation of loci associated with GGT was performed using the FUMA (v1.3.5) web-based platform (ref. 43). Publicly available GWAS summary statistics on GGT from the Neale Lab (UK Biobank) was used. Genome-wide significant loci were defined as non-overlapping genomic regions that extend across an LD window of $r^2 \geq 0.6$ from the association signals with $P < 5 \times 10^{-8}$. Independent ($r^2 < 0.1$) lead SNPs from each locus were defined as those most strongly associated with the outcome at the specific region. Functional annotation of all candidate risk SNPs was obtained from different repositories integrated in FUMA. These functionally annotated SNPs were mapped to protein-coding genes using the following two strategies: 1) positional mapping, with the maximum distance of 10kb to protein-coding genes and 2) eQTL mapping, using information from GTEx (v8) and cis- eQTLs and trans-eQTLs from eQTLGen (false discovery rate < 0.05) of all independent statistically significant SNPs.

The mapped genes were analyzed using the gene2func module of FUMA, which performs gene set enrichment analysis across biological pathways, canonical pathways, and GWAS catalog phenotypes. Gene sets showing enrichment were identified based on FDR adjusted p-values, and a subset of pathways relevant to insulin metabolism and glucose regulation were highlighted. Tissue-specific differentially expressed gene (DEG) analysis was performed using the gene2func module in FUMA, which integrates GTEx v8 expression data. Genes mapped through positional and eQTL mapping were assessed for upregulated, downregulated, and overall DEG enrichment across 30 GTEx tissues. Significance was determined based on Bonferroni-adjusted p-values as a default method in MAGMA analysis in FUMA.

The objective of the FUMA analysis was to provide biological context for the MR findings by identifying enriched pathways and tissue expression patterns among GGT-associated loci, particularly to evaluate whether these loci are functionally linked to insulin signaling and metabolic regulation.

2.9 Statistical analysis

Differences in the continuous variables between the three groups were tested with non-parametric test Kruskal-Wallis and pairwise comparison was done using t-test or Wilcoxon Signed Rank test, as applicable. Univariate linear regression was used to assess the effect of HbA1c and FBG on liver fat percentage and HOMA-IR on GGT levels, respectively. Multivariate Linear regression was done with the same models to adjust for the effects of other covariates. Lipid profile variables were examined descriptively across groups and did not show substantial differences that would materially influence the observed associations; therefore, they were not included as covariates in the regression models. Information on smoking status was not consistently available across all participants and was therefore not included in the adjusted

models. All tests of significance were two-sided at a significance level of $\alpha = 0.05$. Statistical analysis was done with R (v4.0.3) (ref. 44) programming language unless specifically mentioned.

3. RESULTS

3.1 Type 2 Diabetes as a significant risk factor for hepatic steatosis in the study population

Linear regression was performed on 244 individuals with MRS-measured liver fat. FBG and HbA1c were tested as predictors in univariate and multivariate models adjusted for age, BMI, and sex. (Supplementary Table 2). Individuals receiving antidiabetic medications were excluded from the study to minimize treatment-related confounding.

In multivariable models, HbA1c ($\beta = 1.9$, $P = 2.0 \times 10^{-03}$) and FBG ($\beta = 0.06$, $P = 0.02$) remained significantly associated with hepatic fat percentage. Standardized coefficients confirmed independent associations (HbA1c standardized $\beta = 0.17$, 95% CI = 0.06 to 0.27; FBG standardized $\beta = 0.13$, 95% CI = 0.02 to 0.24). Clinically, this corresponds to an approximate 1.9% increase in liver fat for each 1% increase in HbA1c and a 0.6% increase in liver fat for every 10 mg/dL increase in fasting glucose, independent of age, BMI, and sex (Supplementary Table 2).

3.2 MASLD with Diabetes showed more severe disease phenotype

Histopathological evaluation was performed in a subset of MASLD individuals (n = 138) to describe disease severity across glycemic groups. Among them, 76 belonged to the ND group, 40 to the PD group, and 22 to the D group. Descriptive analysis demonstrated a higher proportion of advanced disease features in the D group compared with PD and ND groups.

The D group had 45.5% of individuals with MASH [NAFLD Activity Score(NAS) > 3], compared with 32.5% in PD and 27.6% in ND (Figure 1B). Similarly, the proportions of individual NAS components—including steatosis score (SS), hepatocyte ballooning score (HBS), and lobular inflammation score (LIS)—were descriptively greater in the D group (Figure 1B). Severe fibrosis (FIB > 2) was observed in 22.7% of individuals in the D group. These patterns were consistent with higher mean liver stiffness measurement (LSM) values in the D group (Table 1).

These analyses are descriptive and intended to illustrate distributional differences across glycemic strata.

In the validation data**,** 1095 individuals were categorized into the **MASLD** group and the **no-MASLD** group consisted of 1491 individuals. Supplementary Table 3 summarizes the demographic and clinical characteristics of MASLD and no-MASLD individuals, further stratified by glycemic status (ND, PD, D)**. MASLD** group had a higher prevalence of individuals with diabetes (29.68%) as compared to **no-MASLD** group (9.3%).

3.3 Serum gamma glutamyl transferase levels were found to be a significant differentiator of MASLD patients with diabetes

Anthropometric measurements and lipid profile did not show discreet differences among the ND, PD and D groups in people with MASLD (Table 1). Also, there was no significant difference among the most established liver damage markers such as ALT (Alanine Amino Transferase) and AST (Aspartate Amino Transferase). Surprisingly, only GGT (Gamma Glutamyl Transferase) was found to be significantly different in D group compared to both ND and PD groups in MASLD (Figure 1C). Mean GGT level was observed to be 42.61 ± 23.01 U/L in ND

(n=184), 46.16 ± 38.65 U/L in PD (n=85) and 62.34 ± 29.75 U/L in D (n=43) groups of MASLD, as compared to 33.02 ± 16.75 U/L in ND (n=150), 34.22 ± 14.94 U/L in PD and 37.54 ± 15.48 U/L in D groups of no-MASLD (Table 1). In the validation cohort, similar results were observed in case of liver damage markers. Only GGT was found to be significantly elevated in D group of MASLD as compared to the other groups (Figure 2A).

Individuals with alcohol use or secondary causes of steatosis were excluded at study entry, thereby minimizing alcohol-related confounding. To assess whether the observed differences in GGT were independent of demographic and metabolic covariates, we performed multivariable regression analyses as described below.

3.4 HOMA-IR found to be significantly associated with GGT levels

HOMA-IR, which is the most established index for assessing Insulin resistance (IR) in clinical and epidemiological studies, was also found to be significantly higher in D group of MASLD with a mean HOMA-IR value of 4.91 ± 6.92 in our discovery cohort (Figure 1D) and 6.59 ± 3.10 in the validation cohort (Figure 2B), showing a greater burden of Insulin resistance in this group.

To evaluate whether insulin resistance independently explains variation in GGT levels beyond potential confounders, multivariable linear regression analyses were performed adjusting for age, BMI, sex, MASLD status, and diabetes status. Liver fat was not included as a covariate in these models to avoid over-adjustment, as MASLD status already reflects hepatic fat burden.

Multivariable regression showed HOMA-IR as a significant predictor of GGT in both the discovery cohort ($\beta = 2.0$, $P < 0.001$, $N = 391$) (Figure 1E) and the validation cohort ($\beta = 0.41$, $P < 0.001$, $N = 2586$) (Figure 2B) while adjusting for age, BMI, sex, MASLD, and diabetes status.

Although the magnitude of the β coefficients differed between the discovery and validation cohorts, both analyses were performed using identical model specifications and variable scaling. The difference in effect size likely reflects variation in sample size and distributional characteristics of HOMA-IR and GGT between the cohorts rather than differences in modeling strategy.

3.5 Mendelian Randomization Analysis

3.5.1 Univariate Causal effect estimates of Insulin resistance associated traits with GGT levels

A total of 22 SNPs were used as instrumental variables for fasting insulin, 6 for percentage liver fat, 59 for HbA1c, and 45 for fasting glucose (Figure 3). MR-PRESSO analysis did not identify significant outlier SNPs, suggesting no evidence of horizontal pleiotropy influencing the causal estimates. All instruments demonstrated adequate strength (F-statistics >10), with detailed SNP-level information provided in Supplementary Table 1.

Figure 3 displays the estimations of the causal impact of Fasting insulin, Percentage Liver Fat, Fasting Glucose and Glycated hemoglobin levels (HbA1c) on GGT in the form of forest plot, for each exposure utilizing various MR methods. In the IVW method, a significant causal relationship was found in fasting insulin ($\beta = 0.52$, 95% CI = 0.42 to 0.61, $P = 2.11 \times 10^{-26}$) and percentage liver fat ($\beta = 0.06$, 95% CI = 0.04 to 0.08, $P = 3.33 \times 10^{-07}$) with GGT. The MR-Egger and WM methods reached the same conclusion on fasting insulin (MR-Egger: $\beta = 0.37$, 95% CI = 0.09 to 0.64, $P = 1.76 \times 10^{-02}$; WM: $\beta = 0.57$, 95% CI = 0.45 to 0.69, $P = 2.80 \times 10^{-20}$) and percentage liver fat (MR-Egger: $\beta = 0.07$, 95% CI = 0.04 to 0.1, $P = 1.71 \times 10^{-02}$; WM: $\beta = 0.06$, 95% CI = 0.04 to 0.08, $P = 2.63 \times 10^{-07}$) with GGT . However, no significant causal

association was found in HbA1c levels (β = 0.02, 95% CI = -0.13 to 0.18, P = 0.78) and fasting glucose (β = -0.05, 95% CI = -0.22 to 0.13, P = 0.59) with GGT.

3.5.2 Sensitivity Analyses

No evidence of heterogeneity was observed between the genetic IVs for fasting insulin and percentage liver fat (Cochran's Q test P > 0.05) but significant heterogeneity was observed in case of genetic IVs for fasting glucose and HbA1c (Supplementary Table 4). None of the MR-Egger regression intercepts deviated from null, indicating no evidence of horizontal pleiotropy (all intercept P > 0.05) (Supplementary Table 5). Leave-one-out analysis confirmed robust and consistent MR effect estimates (Supplementary Figure 2). In reverse MR analysis, there was no evidence of a causal effect of GGT on each of the four insulin resistance associated traits (Supplementary Table 6). Steiger directionality testing also confirmed that, for all exposures, the genetic variants explained greater variance in the exposure than in GGT (all Steiger P-values < 0.001), supporting the assumed direction of causality (Supplementary Table 7).

To further address potential bias arising from partial sample overlap between the UK Biobank–derived liver fat and GGT GWAS datasets, we applied MRlap correction (ref. 45). Following correction, the association between percentage liver fat and GGT was attenuated and no longer statistically significant (β = 0.097, 95% CI -0.021 to 0.216, P = 0.11), suggesting that the univariable association may have been influenced by overlap-related bias (Supplementary Table 8).

3.5.3 Multivariable MR Analysis

In the multivariable MR (MVMR) analysis, fasting insulin remained significantly associated with GGT levels (β = 0.34, 95% CI = 0.04 to 0.64, P = 0.02), suggesting a potential causal effect

independent of the other metabolic traits. In contrast, fasting glucose (β=0.06, 95% CI = -0.08 to 0.19, P = 0.41) and HbA1c (β = 0.05, 95% CI = -0.13 to 0.22, P = 0.60) did not show significant associations with GGT after adjusting for the effects of fasting insulin and percentage liver fat. While percentage liver fat showed an association with GGT in univariate MR, this effect was attenuated in MVMR (β = 0.06, 95% CI = -0.03 to 0.14, P = 0.18), suggesting that fasting insulin may play a more prominent role in influencing GGT levels than hepatic fat accumulation in the multivariable framework. Conditional F-statistics demonstrated adequate instrument strength for fasting insulin (F = 12.86), fasting glucose (F = 43.05), and HbA1c (F = 32.57). The conditional F-statistic for percentage liver fat was lower (F = 7.77), indicating comparatively weaker instrument strength in the multivariable setting (Table 2). Therefore, the estimated effect of liver fat in the multivariable model should be interpreted with caution. The results of the MVMR are provided in Table 2.

3.6 Functional annotation and pathway enrichment using FUMA

FUMA-based functional mapping of GGT-associated variants identified a total of 1733 protein-coding genes, based on positional mapping, eQTL associations. The details of the genes are provided in Supplementary Table 9. These mapped genes were further examined through gene set enrichment and tissue-specific expression analyses using Gene2Func module of FUMA, with the objective of providing biological context for the MR findings.

The results of pathway enrichment analysis showed that genes linked to GGT were significantly enriched in insulin-related and metabolic pathways (FDR-adjusted P < 0.05). The top enriched gene sets included those related to lipid metabolism, type 2 diabetes, fasting insulin regulation, glucose homeostasis, and *PI3K/AKT* signaling (Figure 4A). Gene-level analysis revealed that several key metabolic regulators contributed repeatedly across enriched pathways, including

GCKR, PPARG, HNF4A, SLC2A2, PTEN, RREB1, GLIS3, and *PROX1*. A detailed list of enriched metabolism-related pathways and their overlapping genes is provided in Supplementary Table 10.

Differential expression analysis using the Gene2Func module highlighted significant tissue-specific expression patterns. The strongest enrichment was observed in liver tissue, consistent with the hepatic origin of GGT. Enrichment was also detected in pancreas and gastrointestinal tissues (Figure 4B).

4. Discussion:

MASLD and T2D are closely related metabolic diseases that often co-occur and share mechanisms like insulin resistance and hepatic lipid accumulation (ref. 46). Consistent with earlier reports (ref. 8-10), we found a high MASLD prevalence (76.7%) in T2D, confirming their strong association. Individuals with MASLD or T2D often show elevated liver enzymes like ALT and AST (ref. 47). However, the clinical relevance of gamma-glutamyl transferase (GGT), another marker of hepatocellular injury and oxidative stress (ref. 48), remains comparatively underexplored.

In this study, we integrated clinical phenotyping, Mendelian Randomization (MR), and functional annotation of GWAS loci to investigate the relationship between insulin resistance related traits, hepatic fat accumulation, and GGT levels in the context of MASLD.

Our clinical results highlight increased metabolic burden in individuals with both MASLD and T2D, marked by significantly higher GGT and HOMA-IR compared to either condition alone (Figure 1). The NHANES dataset replicated these findings, reinforcing their robustness (Figure

2). This consistency across independent cohorts supports the potential role of GGT as a biomarker reflecting metabolic stress associated with insulin resistance in MASLD.

To overcome the shortcomings of observational associations and estimate potential causality, we carried out Mendelian Randomization (MR), using genetic instruments of insulin resistance-related traits. In univariable MR, both fasting insulin and percentage liver fat had significant causal effects on the level of GGT, which indicates that both insulin resistance and hepatic lipid deposition could be independent contributors to GGT increase (Figure 3). However, in multivariable MR, only fasting insulin retained significance (Table 2). These findings suggest that genetically predicted fasting insulin may play a more direct role in influencing GGT levels than hepatic fat accumulation when these exposures are considered simultaneously. However, given the comparatively lower instrument strength for percentage liver fat in the multivariable MR model (conditional F = 7.77), this comparison should be interpreted with caution. No significant causal effects were observed for fasting glucose and HbA1c suggesting that markers reflecting glycemic control may be less directly associated with GGT levels than traits related to insulin resistance (Figure 3).

Insulin resistance may enhance GGT expression via oxidative stress, glutathione metabolism, and disrupted hepatic insulin signaling. Disruption of insulin signaling pathways may promote oxidative stress and metabolic imbalance in hepatocytes, leading to compensatory upregulation of GGT to maintain glutathione homeostasis (ref. 49-51). These mechanisms provide a plausible biological link between insulin resistance and elevated GGT levels in metabolic liver disease. To further explore the biological basis of these findings, we performed gene-set enrichment and tissue-specific expression analysis using FUMA. Gene-set enrichment analysis indicated significant enrichment of pathways related to lipid metabolism, insulin signaling, and glucose

homeostasis among GGT-associated loci. Among the top gene sets were genes for fasting insulin, type 2 diabetes, *PI3K-AKT* signaling, and lipid binding (Figure 4). Gene-level analysis further identified several genes repeatedly contributing to these enriched pathways, including *GCKR, PPARG, HNF4A, SLC2A2, PTEN, RREB1, GLIS3, and PROX1* (Supplementary Table 10), many of which have established roles in metabolic regulation and glucose homeostasis (ref. 52, 53). All of these results suggest that the increase in GGT levels seen in individuals with MASLD is not simply due to steatosis and inflammation, but rather a systemic metabolic dysfunction, especially in relation to the insulin signaling system.

Tissue expression analysis showed GGT-linked genes were predominantly expressed in the liver, consistent with GGT's hepatic origin (Figure 4). Enrichment was also observed in pancreas and gastrointestinal tissues (Figure 4), suggesting that these genes may be expressed within broader metabolic and endocrine regulatory networks.

Together, our findings support that GGT is not simply a downstream marker of liver injury but also reflects upstream metabolic dysfunction, particularly insulin resistance. The use of MR to establish a directional and causal link between fasting insulin and GGT provides critical support for this interpretation and also mitigates concerns about reverse causality or residual confounding. Clinically, these findings support GGT as a marker reflecting insulin resistance–related metabolic stress in MASLD. However, further prospective and interventional studies are required to establish its role as a predictive or clinically actionable biomarker. These results suggest that insulin resistance may be more strongly associated with GGT levels than hepatic fat in MASLD, although this should be interpreted with caution.

Despite the strengths of our study, including multi-cohort validation and integrative functional annotation, certain limitations must be acknowledged. The cross-sectional design of the clinical

component limits causal inference, though this is addressed through the application of MR. Histological data for liver fibrosis or inflammation were not available in all participants, which may constrain phenotypic resolution. An additional consideration is the difference in hepatic fat assessment methods across datasets. In the clinical cohort, hepatic steatosis was evaluated using ultrasonography and H^1-MRS, whereas the MR analysis utilized MRI-based PDFF measurements from the UK Biobank GWAS. MRI-PDFF provides quantitative and highly sensitive assessment of hepatic fat, while ultrasound is semi-quantitative and less sensitive for mild steatosis. However, both modalities capture hepatic fat accumulation as the underlying biological phenotype. Importantly, the MR analysis estimates genetically predicted liver fat independent of measurement modality, thereby reflecting lifelong predisposition rather than cross-sectional imaging variation. Differences in measurement techniques may influence direct comparability of effect sizes and should be considered when interpreting the findings. Another limitation relates to the ancestry of the GWAS datasets used for MR analysis. The exposure and outcome GWAS were primarily derived from individuals of European ancestry, whereas the clinical cohort consisted of individuals of Indian origin. Although genetic effects for metabolic traits are generally consistent across populations, differences in allele frequencies or linkage disequilibrium patterns may influence transferability of genetic instruments. In addition, while multiple sensitivity analyses were performed to assess potential pleiotropy, including MR-Egger and leave-one-out analyses, the possibility of residual horizontal pleiotropy cannot be completely excluded. Finally, the number of instrumental variants available for certain exposures, particularly percentage liver fat, was relatively limited, which may reduce statistical power in multivariable MR models.

Acknowledgements:

The authors would like to acknowledge all the study participants involved in this study. We acknowledge the support of the BRIC- National Institute of Biomedical Genomics (NIBMG) and the Institute of Post Graduate Medical Education and Research (IPGMER) in conducting our research. The facilities provided by these two institutes were instrumental in carrying out our experiments and collecting the data necessary for this study. We would like to acknowledge the support of the Indian Council of Medical Research (ICMR), Government of India, for providing fellowship [Fellowship Number: 3/1/3/JRF-2021/HRD-033(1211840)] to Mr. Ayan Mandal as an ICMR-JRF.

Author Contribution:

AM was responsible for designing the study, performing data analysis, conducting Mendelian Randomization and functional genomics analyses, interpreting results, and writing the initial draft of the manuscript. AC was responsible for sample collection, data generation, interpretation of results and manuscript preparation. DG contributed to statistical analysis, data visualization, and assisted in refining the analysis pipeline and figures. BM contributed to statistical analysis. AB supervised genomic data integration and contributed to interpreting genetic findings. PB conceptualized and supervised the overall study, secured ethical approvals, interpreted the findings, and contributed to writing and revising the manuscript. All authors reviewed and approved the final version of the manuscript.

Competing Interests:

The authors declare no competing interests

Data Availability Statement:

The clinical dataset generated and analyzed in this study is available from the corresponding author upon reasonable request due to participant privacy restrictions. Publicly available datasets were also used in this study. The NHANES 2017–2020 pre-pandemic dataset is available from the Centers for Disease Control and Prevention (CDC) website (https://www.cdc.gov/nchs/nhanes). GWAS summary statistics for fasting insulin, fasting glucose, and glycated hemoglobin (HbA1c) were obtained from the MAGIC consortium via the NHGRI-EBI GWAS Catalog with accession numbers GCST90002238, GCST90002232, and GCST90002244, respectively. Summary statistics for MRI-derived liver fat were obtained from the UK Biobank GWAS (accession GCST90016673). GWAS summary statistics for gamma-glutamyl transferase (GGT) were obtained from the UK Biobank Neale Lab release (field ID: 30730_irnt).

Ethical Statement:

The study was done following the guidelines of the 1975 Declaration of Helsinki and its revisions. The study was approved by the Institutional Ethical Committee of National Institute of Biomedical Genomics, Kalyani. Participants were recruited in the study with informed consent (Ethical clearance number: NIBMG/2012/1/6, dated on January 6, 2012).

Code Availability statement:

All statistical analyses were conducted using R (v4.0.3) using the TwoSampleMR (v0.6.30), MendelianRandomization (v0.10.0), and MVMR (v0.4.2) packages. The scripts used to perform the analyses are available from the corresponding author upon reasonable request**.**

References:

1. Eslam M, Sanyal AJ, George J, Sanyal A, Neuschwander-Tetri B, Tiribelli C *et al.* MAFLD: A Consensus-Driven Proposed Nomenclature for Metabolic Associated Fatty Liver Disease. *Gastroenterology* 2020; **158**. https://doi.org/10.1053/j.gastro.2019.11.312.

2. Younossi ZM, Koenig AB, Abdelatif D, Fazel Y, Henry L, Wymer M. Global epidemiology of nonalcoholic fatty liver disease—Meta-analytic assessment of prevalence, incidence, and outcomes. *Hepatology* 2016; **64**. https://doi.org/10.1002/hep.28431.

3. Kleiner DE, Makhlouf HR. Histology of Nonalcoholic Fatty Liver Disease and Nonalcoholic Steatohepatitis in Adults and Children. Clin Liver Dis. 2016; **20**. https://doi.org/10.1016/j.cld.2015.10.011.

4. Lazarus J V., Mark HE, Anstee QM, Arab JP, Batterham RL, Castera L *et al.* Advancing the global public health agenda for NAFLD: a consensus statement. Nat Rev Gastroenterol Hepatol. 2022; **19**. https://doi.org/10.1038/s41575-021-00523-4.

5. Shalimar, Elhence A, Bansal B, Gupta H, Anand A, Singh TP *et al.* Prevalence of Non-alcoholic Fatty Liver Disease in India: A Systematic Review and Meta-analysis. *J Clin Exp Hepatol* 2022; **12**. https://doi.org/10.1016/j.jceh.2021.11.010.

6. Rinella ME, Lazarus J V., Ratziu V, Francque SM, Sanyal AJ, Kanwal F *et al.* A multisociety Delphi consensus statement on new fatty liver disease nomenclature. Ann Hepatol. 2024; **29**. https://doi.org/10.1016/j.aohep.2023.101133.

7. Aller de la Fuente R, Mora Cuadrado N, Tafur C, López Gómez JJ, Gómez de la Cuesta S, García Sánchez MC *et al.* Histopathological differences in patients with biopsy-proven non-

alcoholic fatty liver disease with and without type 2 diabetes. *Endocrinol Diabetes Nutr* 2018; **65**. https://doi.org/10.1016/j.endinu.2017.12.011.

8. Forlano R, Stanic T, Jayawardana S, Mullish BH, Yee M, Mossialos E *et al.* A prospective study on the prevalence of MASLD in people with type-2 diabetes in the community. Cost effectiveness of screening strategies. *Liver International* 2024; **44**. https://doi.org/10.1111/liv.15730.

9. Ajmera V, Cepin S, Tesfai K, Hofflich H, Cadman K, Lopez S *et al.* A prospective study on the prevalence of NAFLD, advanced fibrosis, cirrhosis and hepatocellular carcinoma in people with type 2 diabetes. *J Hepatol* 2023; **78**. https://doi.org/10.1016/j.jhep.2022.11.010.

10. En Li Cho E, Ang CZ, Quek J, Fu CE, Lim LKE, Heng ZEQ *et al.* Global prevalence of non-alcoholic fatty liver disease in type 2 diabetes mellitus: An updated systematic review and meta-analysis. *Gut* 2023; **72**. https://doi.org/10.1136/gutjnl-2023-330110.

11. Zoppini G, Fedeli U, Gennaro N, Saugo M, Targher G, Bonora E. Mortality from chronic liver diseases in diabetes. *American Journal of Gastroenterology* 2014; **109**. https://doi.org/10.1038/ajg.2014.132.

12. Khan RMM, Chua ZJY, Tan JC, Yang Y, Liao Z, Zhao Y. From pre-diabetes to diabetes: Diagnosis, treatments and translational research. Medicina (Lithuania). 2019; **55**. https://doi.org/10.3390/medicina55090546.

13. Vesa C, Behl T, Nemeth S, Bratu O, Diaconu C, Moleriu R *et al.* Prediction of NAFLD occurrence in prediabetes patients. *Exp Ther Med* 2020; **20**. https://doi.org/10.3892/etm.2020.9320.

14. Kumar P, Rawat S, Kakar A, Sinha A. Prevalence of non-alcoholic fatty liver disease among diabetes, prediabetes and healthy population. *J Family Med Prim Care* 2022; **11**. https://doi.org/10.4103/jfmpc.jfmpc_856_22.

15. Tilg H, Moschen AR, Roden M. NAFLD and diabetes mellitus. Nat Rev Gastroenterol Hepatol. 2017; **14**. https://doi.org/10.1038/nrgastro.2016.147.

16. Li M, Zhang S, Wu Y, Ye J, Cao X, Liu J *et al.* Prevalence of Insulin Resistance in Subjects with Nonalcoholic Fatty Liver Disease and Its Predictors in a Chinese Population. *Dig Dis Sci* 2015; **60**. https://doi.org/10.1007/s10620-015-3564-5.

17. Cai X, Gao J, Hu J, Wen W, Zhu Q, Wang M *et al.* Dose-Response Associations of Metabolic Score for Insulin Resistance Index with Nonalcoholic Fatty Liver Disease among a Nonobese Chinese Population: Retrospective Evidence from a Population-Based Cohort Study. *Dis Markers* 2022; **2022**. https://doi.org/10.1155/2022/4930355.

18. Wang M, Zhao Y, He Y, Zhang L, Liu J, Zheng S *et al.* The bidirectional relationship between NAFLD and type 2 diabetes: A prospective population-based cohort study. *Nutrition, Metabolism and Cardiovascular Diseases* 2023; **33**. https://doi.org/10.1016/j.numecd.2023.05.018.

19. Brennan PN, Dillon JF, Tapper EB. Gamma-Glutamyl Transferase (γ-GT) - an old dog with new tricks? Liver Int. 2022;**42**. https://doi.org/10.1111/liv.15099.

20. Kunutsor SK, Abbasi A, Adler AI. Gamma-glutamyl transferase and risk of type II diabetes: an updated systematic review and dose-response meta-analysis. Ann Epidemiol. 2014; **24**. https://doi.org/10.1016/j.annepidem.2014.09.001.

21. Shin JY, Chang SJ, Shin YG, Seo KS, Chung CH. Elevated serum gamma-glutamyltransferase levels are independently associated with insulin resistance in non-diabetic subjects. Diabetes Res Clin Pract. 2009; **84**. https://doi.org/10.1016/j.diabres.2009.02.004.

22. Kunutsor SK, Bakker SJ, Kootstra-Ros JE, Gansevoort RT, Dullaart RP. Circulating gamma glutamyltransferase and prediction of cardiovascular disease. Atherosclerosis. 2015 ; **238**. https://doi.org/10.1016/j.atherosclerosis.2014.12.045.

23. Chatterjee A, Basu A, Das K, Chowdhury A, Basu P. Exome-wide scan identifies significant association of rs4788084 in IL27 promoter with increase in hepatic fat content among Indians. *Gene* 2021; **775**. https://doi.org/10.1016/j.gene.2021.145431.

24. Matthews DR, Hosker JP, Rudenski AS, Naylor BA, Treacher DF, Turner RC. Homeostasis model assessment: insulin resistance and β-cell function from fasting plasma glucose and insulin concentrations in man. *Diabetologia* 1985; **28**. https://doi.org/10.1007/BF00280883.

25. Berzigotti A, Tsochatzis E, Boursier J, Castera L, Cazzagon N, Friedrich-Rust M *et al.* EASL Clinical Practice Guidelines on non-invasive tests for evaluation of liver disease severity and prognosis – 2021 update. *J Hepatol* 2021; **75**. https://doi.org/10.1016/j.jhep.2021.05.025.

26. Brunt EM, Kleiner DE, Wilson LA, Belt P, Neuschwander-Tetri BA. Nonalcoholic fatty liver disease (NAFLD) activity score and the histopathologic diagnosis in NAFLD: Distinct clinicopathologic meanings. *Hepatology* 2011; **53**. https://doi.org/10.1002/hep.24127.

27. Kleiner DE, Brunt EM, Van Natta M, Behling C, Contos MJ, Cummings OW *et al.* Design and validation of a histological scoring system for nonalcoholic fatty liver disease. *Hepatology* 2005; **41**. https://doi.org/10.1002/hep.20701.

28. Skrivankova VW, Richmond RC, Woolf BAR, Yarmolinsky J, Davies NM, Swanson SA *et al.* Strengthening the Reporting of Observational Studies in Epidemiology Using Mendelian Randomization: The STROBE-MR Statement. *JAMA - Journal of the American Medical Association* 2021; **326**. https://doi.org/10.1001/jama.2021.18236.

29. Sevilla-González M, Smith K, Wang N, Jensen AE, Manning AK *et al*. Heterogeneous effects of genetic variants and traits associated with fasting insulin on cardiometabolic outcomes. Nat Commun. 2025; **16**. https://doi.org/10.1038/s41467-025-57452-y.

30. Sherwani SI, Khan HA, Ekhzaimy A, Masood A, Sakharkar MK. Significance of HbA1c Test in Diagnosis and Prognosis of Diabetic Patients. Biomark Insights. 2016; **11**. https://doi.org/10.4137/BMI.S38440.

31. Chen J, Spracklen CN, Marenne G, Varshney A, Corbin LJ, Luan J *et al.* The trans-ancestral genomic architecture of glycemic traits. *Nat Genet* 2021; **53**. https://doi.org/10.1038/s41588-021-00852-9.

32. Liu Y, Basty N, Whitcher B, Bell JD, Sorokin EP, van Bruggen N *et al.* Genetic architecture of 11 organ traits derived from abdominal MRI using deep learning. *Elife* 2021; **10**. https://doi.org/10.7554/eLife.65554.

33. Saravia G, Civeira F, Hurtado-Roca Y, Andres E, Leon M, Laclaustra M *et al*. Glycated Hemoglobin, Fasting Insulin and the Metabolic Syndrome in Males. Cross-Sectional

Analyses of the Aragon Workers' Health Study Baseline. *PLoS One*. 2015; **10**. https://doi.org/10.1371/journal.pone.0132244.

34. Albai O, Braha A, Timar R, Lazar S, Popescu S, Timar B. Markers Of Insulin Resistance and Their Clinical Implications In Patients with Type 2 Diabetes and Metabolic Dysfunction-Associated Steatotic Liver Disease. *Diabetes, Metabolic Syndrome and Obesity: Targets and Therapy*. 2026; **19**. https://doi.org/10.2147/DMSO.S577797.

35. 1000 Genomes Project Consortium; Auton A, Brooks LD, Durbin RM, Garrison EP, Kang HM *et al*. A global reference for human genetic variation. *Nature*. 2015; **526**. https://doi.org/10.1038/nature15393.

36. Verbanck M, Chen CY, Neale B, Do R. Detection of widespread horizontal pleiotropy in causal relationships inferred from Mendelian randomization between complex traits and diseases. *Nat Genet* 2018; **50**. https://doi.org/10.1038/s41588-018-0099-7.

37. Burgess S, Butterworth A, Thompson SG. Mendelian randomization analysis with multiple genetic variants using summarized data. *Genet Epidemiol* 2013; **37**. https://doi.org/10.1002/gepi.21758.

38. Bowden J, Smith GD, Burgess S. Mendelian randomization with invalid instruments: Effect estimation and bias detection through Egger regression. *Int J Epidemiol* 2015; **44**. https://doi.org/10.1093/ije/dyv080.

39. Bowden J, Davey Smith G, Haycock PC, Burgess S. Consistent Estimation in Mendelian Randomization with Some Invalid Instruments Using a Weighted Median Estimator. *Genet Epidemiol* 2016; **40**. https://doi.org/10.1002/gepi.21965.

40. Sanderson E, Spiller W, Bowden J. Testing and correcting for weak and pleiotropic instruments in two-sample multivariable Mendelian randomization. *Statistics in Medicine*. 2021; **40**. https://doi.org/10.1002/sim.9133.

41. Hartwig FP, Davies NM, Hemani G, Davey Smith G. Two-sample Mendelian randomization: avoiding the downsides of a powerful, widely applicable but potentially fallible technique. *Int J Epidemiol*. 2016; **45**. https://doi.org/10.1093/ije/dyx028.

42. Yavorska OO, Burgess S. MendelianRandomization: an R package for performing Mendelian randomization analyses using summarized data. *Int J Epidemiol*. 2017; **46**. https://doi.org/10.1093/ije/dyx034.

43. Watanabe K, Taskesen E, Van Bochoven A, Posthuma D. Functional mapping and annotation of genetic associations with FUMA. *Nat Commun* 2017; **8**. https://doi.org/10.1038/s41467-017-01261-5.

44. Ihaka R, Gentleman R. R: A Language for Data Analysis and Graphics. *Journal of Computational and Graphical Statistics* 1996; **5**. https://doi.org/10.1080/10618600.1996.10474713.

45. Mounier N, Kutalik Z. Bias correction for inverse variance weighting Mendelian randomization. *Genet Epidemiol*. 2023; **47**. https://doi.org/10.1002/gepi.22522.

46. Ciardullo S, Vergani M, Perseghin G. Nonalcoholic Fatty Liver Disease in Patients with Type 2 Diabetes: Screening, Diagnosis, and Treatment. J Clin Med. 2023; **12**. https://doi.org/10.3390/jcm12175597.

47. Dai CY, Fang TJ, Hung WW, Tsai HJ, Tsai YC. The Determinants of Liver Fibrosis in Patients with Nonalcoholic Fatty Liver Disease and Type 2 Diabetes Mellitus. *Biomedicines* 2022; **10**. https://doi.org/10.3390/biomedicines10071487.

48. Kunutsor SK. Gamma-glutamyltransferase—friend or foe within? Liver International. 2016; **36**. https://doi.org/10.1111/liv.13221.

49. Petersen MC, Shulman GI. Mechanisms of insulin action and insulin resistance. Physiol Rev. 2018; **98**. https://doi.org/10.1152/physrev.00063.2017.

50. Mitrić A, Castellano I. Targeting gamma-glutamyl transpeptidase: A pleiotropic enzyme involved in glutathione metabolism and in the control of redox homeostasis. Free Radic Biol Med. 2023; **208**. https://doi.org/10.1016/j.freeradbiomed.2023.09.020.

51. Lu SC. Glutathione synthesis. Biochim Biophys Acta Gen Subj. 2013; **1830**. https://doi.org/10.1016/j.bbagen.2012.09.008.

52. Scott, R., Lagou, V., Welch, R. *et al.* Large-scale association analyses identify new loci influencing glycemic traits and provide insight into the underlying biological pathways. *Nat Genet.* 2012; **44**. https://doi.org/10.1038/ng.2385.

53. Sladek, R., Rocheleau, G., Rung, J. *et al.* A genome-wide association study identifies novel risk loci for type 2 diabetes. *Nature.* 2007; **445**. https://doi.org/10.1038/nature05616.

Figure Legends:

Figure 1 : **A)** Schematic representation of study design for categorizing participants in the discovery cohort (N = 498) into MASLD (N = 312) and no-MASLD (N = 186) groups, further stratified by diabetes status: no-diabetes (ND), prediabetes (PD), and diabetes (D).

B) Stacked bar plots showing the distribution of MASLD severity grades across ND, PD, and D groups.

C) Violin plots of serum GGT levels in MASLD and no-MASLD groups stratified by ND, PD, and D status.

D) Violin plots of HOMA-IR levels in MASLD and no-MASLD groups across the three diabetes status categories.

E) Scatter plot showing the relationship between serum GGT and HOMA-IR levels, with a fitted linear regression line. The regression model was adjusted for age, BMI, sex, MASLD status, and diabetes status.

Figure 2: **A)** Violin plots showing serum levels of liver damage markers—ALT, AST, and GGT—in MASLD and no-MASLD groups stratified by diabetes status: ND, PD and D in the validation cohort. Statistical significance between subgroups was assessed using the Kruskal–Wallis test.

B) Violin plots depicting HOMA-IR levels across ND, PD, and D subgroups within MASLD and no-MASLD groups. A linear regression analysis was performed to assess the association between serum GGT and HOMA-IR levels, adjusted for age, BMI, sex, MASLD status, and diabetes status in the validation cohort.

Figure 3: Forest plot showing the causal effects of four metabolic risk factors—fasting insulin, percent liver fat, glycated hemoglobin (HbA1c), and fasting glucose—on serum GGT levels, as estimated using univariate Mendelian Randomization (MR). Three MR methods were applied: inverse variance weighted (IVW), MR Egger, and weighted median. The x-axis represents the beta estimate for GGT per standard deviation (SD) increase in each risk factor, with corresponding 95% confidence intervals. Significant associations were observed for fasting insulin and percent liver fat, indicating a potential causal effect on GGT levels

Figure 4: A) Gene set enrichment analysis (GSEA) results from FUMA using genes associated with GGT levels. The top enriched gene sets include insulin signaling, glucose metabolism, lipid binding, and type 2 diabetes–related pathways, highlighting the metabolic relevance of GGT-associated loci.

B) Tissue-specific expression analysis using the gene2func module in FUMA, showing differentially expressed genes (DEGs) across multiple tissue types. Notably, GGT-associated genes were significantly upregulated in liver, pancreas, and stomach tissues, indicating their functional relevance in metabolic regulation. Significant tissues, after multiple testing corrections are shown in red

Table Legends:

Table 1: Comparison of clinicopathological characteristics among study groups in the discovery cohort

Table 2: Multivariable MR results for glycemic traits and liver fat on GGT levels

Table 1: Comparison of clinicopathological characteristics among study groups in the discovery cohort

Parameters	MASLD(N=312)				no_MASLD(N=186)			
	ND N = 184	**PD N = 85**	**D N = 43**	**p-value**	**ND N = 150**	**PD N = 23**	**D N = 13**	**p-value**
age	40 (11)	46 (9)	43 (11)	<0.001	40 (12)	46 (14)	51 (9)	0.001
BMI	26.6 (3.9)	26.9 (3.5)	26.6 (4.2)	0.6	21.6 (4.1)	22.6 (3.7)	20.8 (2.8)	0.3
SEX				0.6				0.3
Male	96 (52%)	39 (46%)	23 (53%)		80 (53%)	16 (70%)	7 (54%)	
Female	88 (48%)	46 (54%)	20 (47%)		70 (47%)	7 (30%)	6 (46%)	
Height(cm)	158 (9)	156 (8)	156 (10)	0.13	158 (10)	160 (11)	158 (11)	0.5
Weight(kg)	67 (10)	66 (8)	65 (13)	0.6	54 (11)	58 (11)	53 (12)	0.2
Hip circumference(cm)	99 (9)	100 (7)	101 (10)	0.4	93 (8)	93 (4)	86 (6)	0.036
Waist Circumference(cm)	92 (8)	93 (8)	94 (10)	0.2	80 (12)	85 (10)	81 (9)	0.13
ALT(U/L)	51 (35)	46 (34)	51 (33)	0.4	32 (20)	39 (31)	23 (8)	0.036
AST(U/L)	40 (24)	38 (20)	45 (26)	0.072	31 (10)	32 (12)	25 (6)	0.034
GGT(U/L)	43 (23)	46 (39)	62 (30)	<0.001	33 (17)	34 (15)	38 (15)	0.4
Triglyceride(mg/dL)	162 (94)	156 (103)	201 (159)	0.3	125 (49)	147 (67)	177 (88)	0.016
Total cholesterol(mg/dL)	181 (44)	180 (39)	187 (53)	>0.9	163 (39)	179 (41)	202 (42)	0.002
HDL(mg/dL)	40 (9)	40 (10)	38 (8)	0.7	44 (13)	41 (10)	46 (11)	0.4

LDL(mg/dL)	109 (42)	108 (38)	111 (42)	>0.9	92 (39)	112 (29)	120 (34)	<0.001
VLDL(mg/dL)	31 (12)	30 (13)	34 (17)	0.4	25 (10)	29 (13)	35 (17)	0.054
C-reactive protein(mg/dL)	4.2 (3.5)	4.8 (3.3)	6.0 (4.4)	0.01	3.68 (3.30)	4.78 (4.68)	1.74 (0.69)	0.027
Liver Stiffness measure (K/Pa)	5.48 (1.88)	6.29 (3.68)	8.80 (7.66)	0.001	4.73 (1.79)	4.46 (0.78)	6.89 (5.29)	0.2
Creatinine(mg/dL)	0.98 (0.17)	0.98 (0.16)	0.94 (0.15)	0.4	0.96 (0.18)	1.06 (0.24)	0.96 (0.15)	0.2
HOMAIR	1.66 (1.31)	1.61 (0.73)	4.91 (6.92)	<0.001	1.21 (0.88)	1.21 (0.44)	2.39 (2.43)	0.01

Values are presented as mean (SD) or n (%).

p-values are from Kruskal–Wallis test (for continuous variables) and Pearson's chi-squared test (for categorical variables).

Table 2: Multivariable MR results for glycemic traits and liver fat on GGT levels

S.no	Exposure	Outcome	nSNP	beta	se	P-value	CI(lower)	CI(upper)	Conditional F-statistics
1	Fasting glucose	Gamma glutamyltransferase	40	0.058	0.07	0.409	-0.07929	0.1946	43.04549
2	Fasting insulin	Gamma glutamyltransferase	14	0.343	0.153	0.025	0.04322	0.64295	12.85591
3	Glycated hemoglobin levels	Gamma glutamyltransferase	49	0.047	0.09	0.597	-0.12839	0.22324	32.5658
4	Percent liver fat	Gamma glutamyltransferase	2	0.057	0.042	0.179	-0.02618	0.13999	7.7677

Estimates are adjusted for all included exposures using multivariable MR.

CI: Confidence Interval; se: Standard Error; nSNP: number of Single Nucleotide Polymorphism.

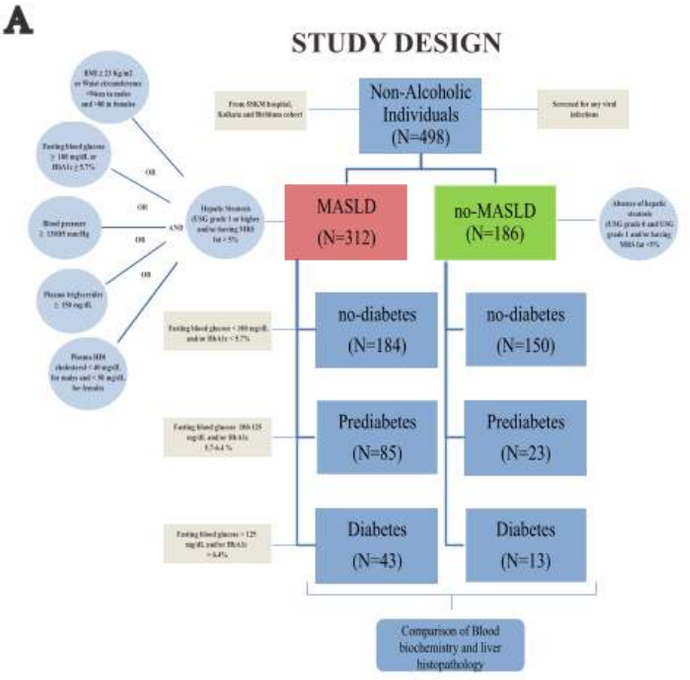

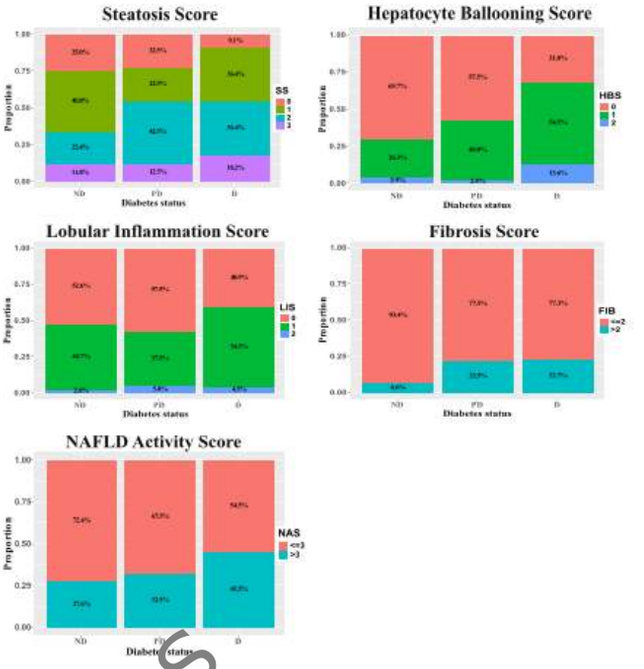

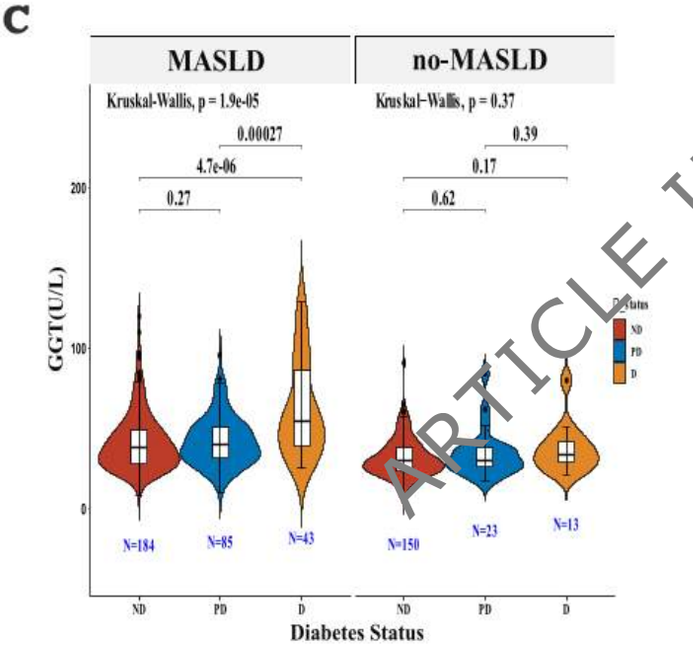

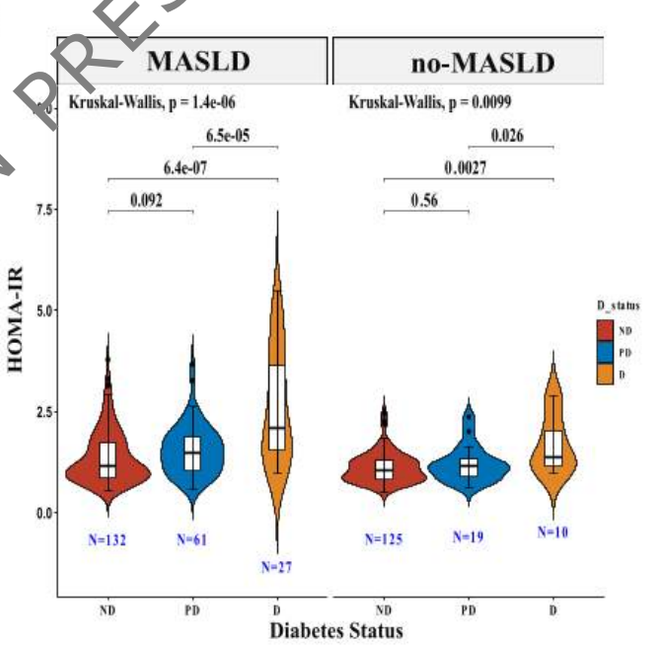

E

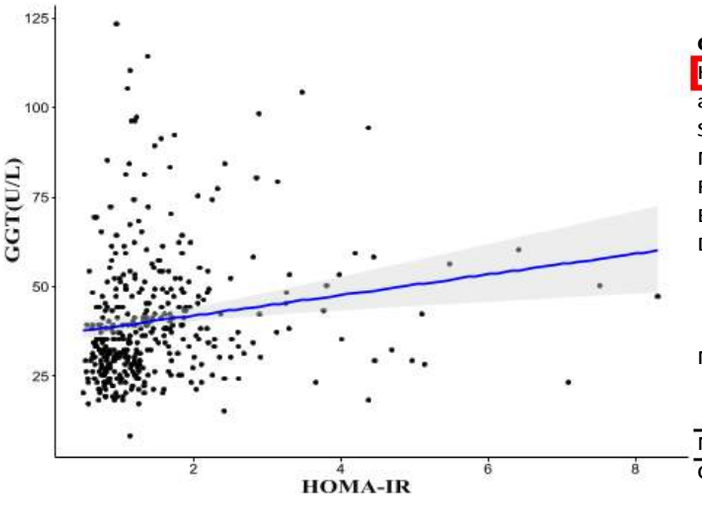

Characteristic	GGT		
	Beta	95% CI	p-value
HOMAIR	2	0.87, 3.2	<0.001
age	-0.14	-0.36, 0.09	0.2
Sex			
Male	—	—	
Female	-7.9	-13, -2.6	0.004
BMI	0.73	0.03, 1.4	0.04
Diabetes Status			
ND	—	—	
PD	3.9	-2.8, 11	0.3
D	13	3.7, 22	0.006
MASLD Status			
no_MASLD	—	—	
MASLD	7.5	1.2, 14	0.02
No. Obs.	391		

CI = Confidence Interval

A.

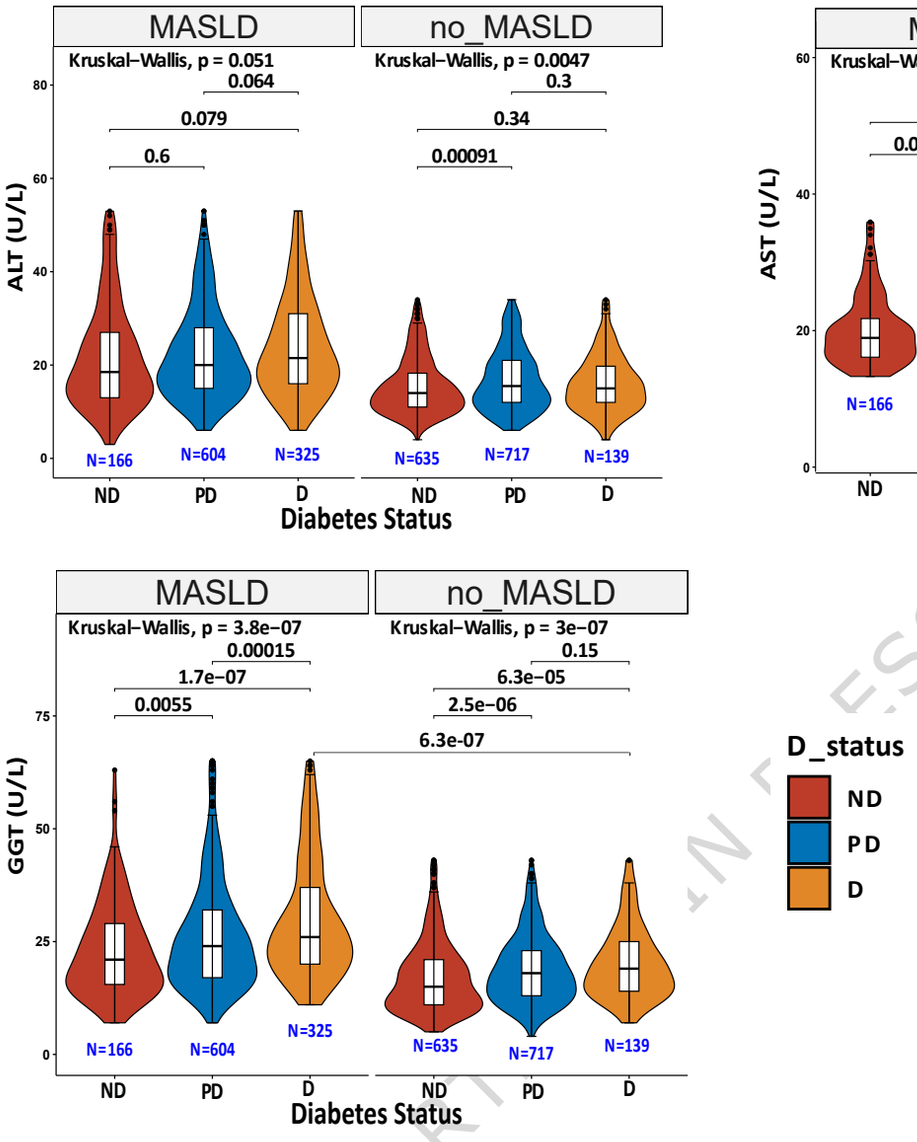

B.

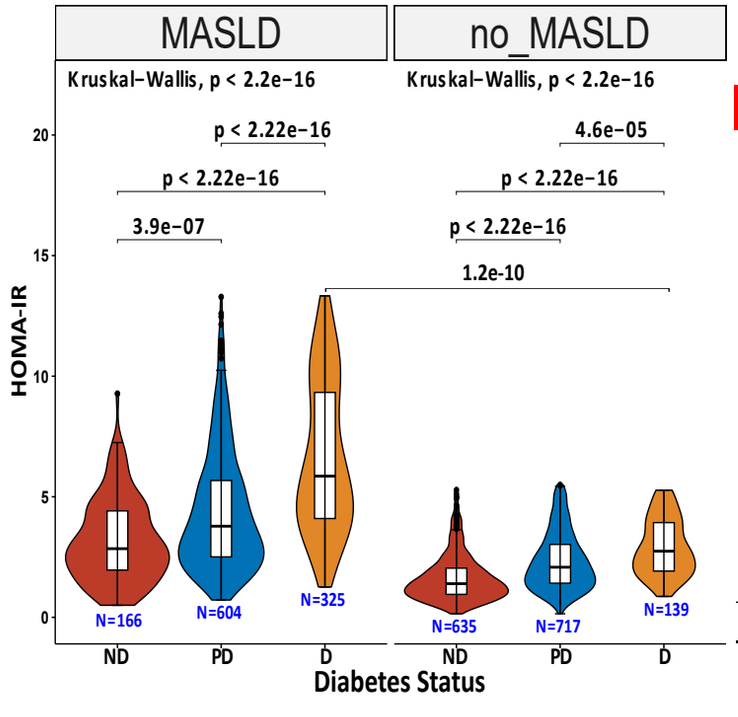

Characteristic	GGT Beta	95% CI	p-value
HOMA-IR	0.41	0.24, 0.57	<0.001
Age	0.04	-0.04, 0.11	0.3
BMI	0.21	0.02, 0.39	0.029
Sex			
Male	—	—	
Female	-7.8	-10, -5.3	<0.001
MASLD status			
no-MASLD	—	—	
MASLD	4.5	1.6, 7.3	0.002
Diabetes status			
ND	—	—	
PD	2.6	-0.51, 5.7	0.1
D	8.4	4.0, 13	<0.001
No. Obs.	2,586		

CI = Confidence Interval

	P-value	No. of IVs	Beta(CI)
Fasting insulin			
Inverse variance weighted	2.11394e−26	22	0.52 (0.42 − 0.61)
MR Egger	1.76382e−02	22	0.37 (0.09 − 0.64)
Weighted median	2.80611e−20	22	0.57 (0.45 − 0.69)
Percent liver fat			
Inverse variance weighted	3.33258e−07	6	0.06 (0.04 − 0.08)
MR Egger	1.71296e−02	6	0.07 (0.03 − 0.1)
Weighted median	2.63377e−07	6	0.06 (0.04 − 0.08)
Glycated hemoglobin levels			
Inverse variance weighted	0.78130	59	0.02 (−0.13 − 0.18)
MR Egger	0.69650	59	0.06 (−0.22 − 0.33)
Weighted median	0.65261	59	0.02 (−0.05 − 0.09)
Fasting glucose			
Inverse variance weighted	0.59698	45	−0.05 (−0.22 − 0.13)
MR Egger	0.99297	45	0 (−0.31 − 0.3)
Weighted median	3.06408e−03	45	0.09 (0.03 − 0.15)

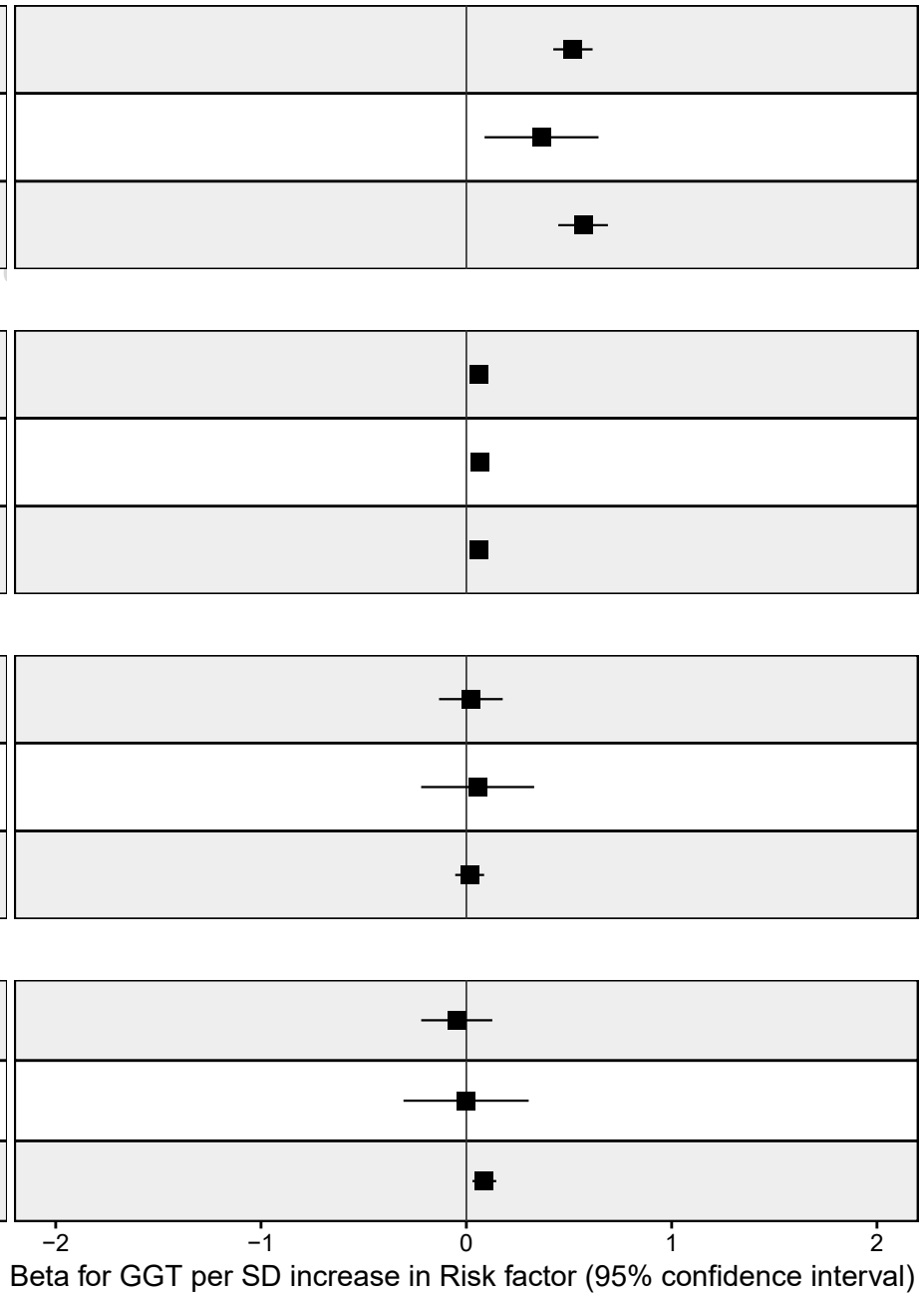

A

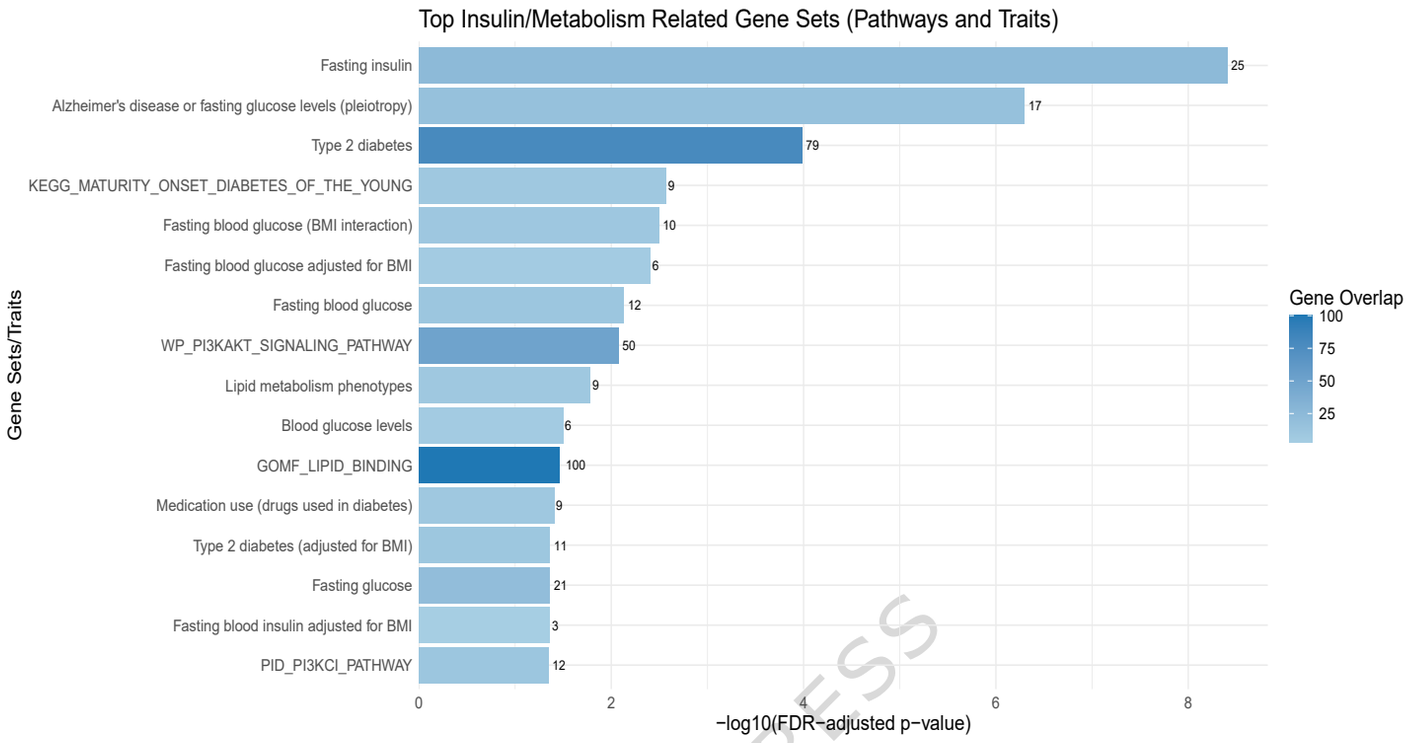

B